



ELSEVIER

Contents lists available at ScienceDirect

## Journal of Ginseng Research

journal homepage: <https://www.sciencedirect.com/journal/journal-of-ginseng-research>

## Research Article

## The anti-tumor efficacy of 20(S)-protopanaxadiol, an active metabolite of ginseng, according to fasting on hepatocellular carcinoma

Wenzhen Li <sup>a,1</sup>, Yifan Wang <sup>a,1</sup>, Xinbo Zhou <sup>a</sup>, Xiaohong Pan <sup>a</sup>, Junhong Lü <sup>a</sup>, Hongliu Sun <sup>a</sup>, Zeping Xie <sup>a</sup>, Shayan Chen <sup>b,c,\*\*</sup>, Xue Gao <sup>a,\*</sup><sup>a</sup> Department of Pharmaceutical Sciences, Binzhou Medical University, Yantai, China<sup>b</sup> Department of Laboratory Science, Tianjin Medical University Nankai Hospital, Tianjin, China<sup>c</sup> Tianjin Key Laboratory of Acute Abdomen Disease Associated Organ Injury and ITCWM Repair, Tianjin Medical University Nankai Hospital, Tianjin, China

## ARTICLE INFO

## Article history:

Received 1 April 2021

Received in revised form

25 May 2021

Accepted 1 June 2021

Available online 10 June 2021

## Keywords:

20(S)-protopanaxadiol  
fasting-mimicking  
intermittent fasting  
hepatocellular carcinoma

## ABSTRACT

**Background:** 20(S)-protopanaxadiol (20(S)-PPD), one of the main active metabolites of ginseng, performs a broad spectrum of anti-tumor effects. Our aims are to search out new strategies to enhance anti-tumor effects of natural products, including 20(S)-PPD. In recent years, fasting has been shown to be multi-functional on tumor progression. Here, the effects of fasting combined with 20(S)-PPD on hepatocellular carcinoma growth, apoptosis, migration, invasion and cell cycle were explored.

**Methods:** CCK-8 assay, trypan blue dye exclusion test, imagings photographed by HoloMonitor™ M4, transwell assay and flow cytometry assay were performed for functional analyses on cell proliferation, morphology, migration, invasion, apoptosis, necrosis and cell cycle. The expressions of genes on protein levels were tested by western blot. Tumor-bearing mice were used to evaluate the effects of intermittent fasting combined with 20(S)-PPD.

**Results:** We firstly confirmed that fasting-mimicking increased the anti-proliferation effect of 20(S)-PPD in human HepG2 cells *in vitro*. In fasting-mimicking culturing medium, the apoptosis and necrosis induced by 20(S)-PPD increased and more cells were arrested at G0-G1 phase. Meanwhile, invasion and migration of cells were decreased by down-regulating the expressions of matrix metalloproteinase (MMP)-2 and MMP-9 in fasting-mimicking medium. Furthermore, the *in vivo* study confirmed that intermittent fasting enhanced the tumor growth inhibition of 20(S)-PPD in H22 tumor-bearing mice without obvious side effects.

**Conclusion:** Fasting significantly sensitized HCC cells to 20(S)-PPD *in vivo* and *in vitro*. These data indicated that dietary restriction can be one of the potential strategies of chinese medicine or its active metabolites against hepatocellular carcinoma.

© 2021 The Korean Society of Ginseng. Publishing services by Elsevier B.V. This is an open access article under the CC BY-NC-ND license (<http://creativecommons.org/licenses/by-nc-nd/4.0/>).

## 1. Introduction

Hepatocellular carcinoma (HCC) is a kind of fatal malignant tumor with metastasis, leading to about 800,000 deaths worldwide annually [1]. Currently, surgical resection is still the optimal therapeutic option against HCC, followed by liver transplantation

and tumor ablation. Due to the absence of early symptoms, about 70%–85% of patients are in advanced stage at the time of diagnosis, with considerably poor prognosis [2]. The vast majority of patients are not appropriate for resection at initial presentation and have to receive cytotoxic chemotherapy for survival. However, in most cases, the clinical effects are not ideal. To date, few molecularly targeted anti-tumor drugs have been developed for HCC. Sorafenib, an oral multi-kinase inhibitor (TKI), was approved by FDA for the treatment of advanced HCC. Nevertheless, it exhibits the moderate efficacy, drug resistance and toxicity with expensive costs [3,4]. There is an urgent need for the development of safe and economical therapeutic approaches against HCC.

Compared to anti-tumor drugs, chinese medicine and its components usually show multiple benefits with minimal side effects,

\* Corresponding author. Department of Pharmaceutical Sciences, Binzhou Medical University, Yantai, China.

\*\* Corresponding author. Department of Laboratory Science, Tianjin Medical University Nankai Hospital, Tianjin, China.

E-mail addresses: [chenshayan@126.com](mailto:chenshayan@126.com) (S. Chen), [042510294@163.com](mailto:042510294@163.com) (X. Gao).

<sup>1</sup> These authors contributed equally to this work.

which make them suitable for patients with advanced HCC. More important, Chinese medicines are cheaper and easily accepted by patients. 20(S)-protopanaxadiol (20(S)-PPD) is one of the characteristic types of triterpenoid saponins in ginsenosides. It is well established that 20(S)-PPD has multi-functions, such as anti-tumor bioactivity. Mechanistically, 20(S)-PPD inhibits tumor cell growth by inducing angiogenesis and delaying metastasis [5,6]. However, it is not yet known whether 20(S)-PPD could be used as an anti-tumor agent in clinical treatment with its higher concentrations of application. Therefore, exploring a potential novel strategy to improve the anti-tumor effects of 20(S)-PPD as well as to reduce the cost of treatments, is necessary.

Fasting is a mode for dietary restriction with several modes, such as intermittent fasting. A substantial emerging evidence has uncovered the therapeutic potential of fasting in cell and animal tumor models. On the basis of these findings, fasting represents a low toxicity or a preferable therapeutic effect [7–9]. However, fasting is still a challenging choice for tumor patients. Long-term fasting can significantly reduce the activity of immune system with no effects to achieve long-term cancer-free survival [10]. It is believed that large-scale trials must be conducted to verify the safety and effectiveness of fasting. At present, the roles and underlying mechanisms of fasting in tumors remain unknown.

Here, using both *in vitro* and *in vivo* hepatocellular carcinoma models, we aim to assess the effects of intermittent fasting and fasting-mimicking in combination with 20(S)-PPD on HCC to maximize therapeutic potential of 20(S)-PPD. This study will also provide some data on the application of fasting in clinical tumor therapy.

## 2. Materials and methods

### 2.1. Reagents

20(S)-PPD was purchased from Meilunbio Corporation (China) and dissolved in dimethyl sulfoxide (DMSO) at 4°C in the dark. RPMI-1640 and fetal bovine serum (FBS) were purchased from Gibco (Grand Island, NJ, USA). CCK-8 detection kit, annexin V-FITC/PI apoptosis detection kit and protein lysis buffer were all purchased from Beyotime Co. Ltd (China). All reagents were of analytical grade. Secondary antibodies coupled to horseradish peroxidase (HRP) were all purchased from Boster Biological Technology Co. Ltd (China).

### 2.2. Cell culture

Human hepatocarcinoma cells were grown in RPMI-1640 medium, supplemented with inactivated FBS (10%) in a humidified incubator of 5% CO<sub>2</sub> at 37°C. Mouse H22 cells were cultured with DMEM medium containing 10% FBS. Cells were cultured in normal medium, containing 2 g/L glucose and 10% FBS, as control groups while cultured in RPMI-1640, containing 0.5 g/L glucose and 1% FBS, for fasting-mimicking groups.

### 2.3. Measurement of cell viability and death

In short, exponentially growing cells were cultured in 96-well plates with 5,000 cells per well. After being treated in the appropriate medium (concentrations of 20(S)-PPD included 0, 5, 10, 20 and 40 μM) for 24 h. Afterwards, 20 μL CCK-8 solution was added to each well for further 4 h. The optical density (OD) values were measured at 450 nm using a microtiter plate reader. At least five replicated wells were carried out for each experiment.

The viability of cells was carried out performing a Trypan Blue Dye Exclusion test. Cells were stained with standard trypan blue

(0.04% in PBS) for 5 min and calculated under a light microscope using a hemocytometer where blue-colored cells were considered as dead cells.

### 2.4. DAPI staining of apoptotic cells

Briefly, cells were rinsed twice with ice-cold PBS buffer and fixed with 4% paraformaldehyde for 15 min. Then, the cell nuclei were counterstained with the 4', 6-diamidino-2-phenylindole (DAPI, 250 ng/mL) in the dark for 15 min. The stained samples were examined under a fluorescent microscope.

### 2.5. Apoptosis and necrosis analysis

Briefly, exponentially growing cells were treated with 20(S)-PPD in control medium and fasting-mimicking medium, respectively. At 24 h treatment, both dead and living cells were collected and then suspended with apoptotic assay buffer. Annexin V-FITC and propidium iodide (PI) dyes were added to each group for 15 min. Then, samples were suspended with PBS buffer and analyzed by a flow cytometry.

### 2.6. Cell cycle analysis

Cell cycle analysis was performed after treatment with control medium or fasting-mimicking medium with several concentrations of 20(S)-PPD for 24 h. Cells were harvested and fixed in 70% ethanol overnight, followed by incubation with 100 μL RNaseA at 37°C for 30 min. Then, cells were stained with PI solution at room temperature for further 30 min in darkness. Cellular fluorescence was measured using a flow cytometry. We evaluated the percentages of cells in each cell cycle phase: G0-G1, S and G2-M.

### 2.7. HoloMonitor™ M4 analysis

The HoloMonitor™ M4 (Phase Holographic Imaging, Lund, Sweden), placed in a standard cell culture incubator, was used to record proliferation, track and related parameters of HepG2 cells which were exposed to 20(S)-PPD in control medium or fasting-mimicking medium in 6-well plates. Imaging was conducted every 30 mins for 24 h and analyzed by HoloMonitor software.

### 2.8. Migration and invasion assay

Cell migration and invasion assays were performed using transwell technique. Cells were pre-treated with 20(S)-PPD in control medium or fasting-mimicking medium for 24 h. Then, serum-deprived cells were plated in the upper chamber. Chamber filters coated with 40 μL Matrigel were used for invasion assay and uncoated filters were used for migration assays. A total of 700 μL medium containing 10% FBS medium was added into the lower chamber. Cells were cultured at 37°C for 24 h, followed by stained with 5% crystal violet and counted under the microscope to evaluate the migration and invasion abilities of cells. All conditions were performed in triplicates and five high-power fields were imaged per replicate.

### 2.9. Western blot analysis

Proteins were loaded on 12% SDS-PAGE gel and electroblotted to polyvinylidene fluoride (PVDF) membranes. Membranes were blocked with 5% non-fat dried milk for 1 h and incubated with the primary antibodies (1:1000) at 4°C overnight. Primary antibodies used for western blot were as follows: rabbit polyclonal antibody CDK2 (PA1547) and rabbit monoclonal antibody β-actin (BM3873)

from Boster Biological Technology co.ltd (Wuhan, China); antibodies against MMP-2 (#87809), cyclin D1 (#55506) and MMP-9 (#2270) were provided by Cell Signaling Technology. Then, horseradish peroxidase-coupled secondary antibodies were used to identified protein-bound primary antibodies at room temperature for 1 h. ECL Plus Western Blot Detection System was performed to detect protein bands according to the manufacturer's instructions (ImageQuant LAS 500, GE Healthcare, USA).  $\beta$ -actin was used as the control and for quantification.

### 2.10. Animal studies

Kunming mice (age, 6 weeks; weight, 20–22 g; female) were obtained from the Qingdao Experimental Animal Center (China) and were fed under specific pathogen free (SPF) condition. Animal protocols were approved by Animal Care and Use Committee of Binzhou Medical University. Mouse H22 cell line ( $1 \times 10^6$  cells) resuspended in 100  $\mu$ L PBS were injected subcutaneously into the right flank of each mouse. 3 days after tumor implantation, the mice were divided in six group ( $n = 5$ ): 20(S)-PPD-low group (30 mg/kg), 20(S)-PPD-low with intermittent fasting group, 20(S)-PPD-middle group (60 mg/kg), 20(S)-PPD-middle with with intermittent fasting group, 20(S)-PPD-high group (100 mg/kg), 20(S)-PPD-high with intermittent fasting group. Mice were treated with 20(S)-PPD, soluted in mixed solvent (anhydrous ethanol: tween 80: saline = 10:1:89, v:v:v), intragastrically every day. During each intermittent fasting period, each mouse was single caged and maintained in standard cages without access to food for 24 hours. Then, mice eat normally for additional 48 hours. All animals had free access to water. Mice were treated for 7 cycles in all. At the time of sacrifice, the spleens, thymes and tumors were collected and weighed. Tumor volumes were calculated using the formula: length  $\times$  width<sup>2</sup>  $\times$  0.5.

### 2.11. Statistical analysis

All of statistical analysis in this study was performed with Graphpad Prism 8.0 software and presented as mean  $\pm$  SD. Comparisons between groups were done with Student's *t* test with the  $P < 0.05$  (\*),  $P < 0.01$  (\*\*) or  $P < 0.001$  (\*\*\*) cutoff for considered significant.

## 3. Results

### 3.1. Fasting-mimicking enhanced the anti-proliferation effect of 20(S)-PPD in human hepatocellular carcinoma cell line HepG2

As a first step, we performed a dose-response curve in order to establish the effect of fasting-mimicking combined with 20(S)-PPD on the cell proliferation capacity. No significant effect on cell proliferation was observed between control medium and fasting-mimicking medium without 20(S)-PPD. The IC<sub>50</sub> value of 20(S)-PPD on HepG2 cells for 24 h treatment was  $62.68 \pm 5.03 \mu$ M in control medium. Of note, as shown in Fig. 1A, when 20(S)-PPD was added in fasting-mimicking medium, cells showed more sensitive to 20(S)-PPD and the IC<sub>50</sub> value of 20(S)-PPD decreased to  $8.32 \pm 1.85 \mu$ M. The results showed that fasting-mimicking in combination with 20(S)-PPD reduced the viability rate in HepG2 cells, indicating that fasting-mimicking could increase the anti-proliferation activity of 20(S)-PPD *in vitro*. Under a microscope, it presented an evident decrease in viability by 20(S)-PPD in fasting-mimicking medium, compared versus in the control medium (Fig. 1B).

On the other hand, results from trypan blue dye exclusion assay demonstrated that the cell death induction of 20(S)-PPD was

significantly increased in fasting-mimicking medium as compared with that in the control medium (Fig. 1C). Fluorescence was observed by DAPI staining, it is obvious that the number of dead cells with a disturbed mass-like morphology in groups treated with 20(S)-PPD-only group was lower than those in groups treated with fasting-mimicking and 20(S)-PPD combined group (Fig. 1D).

### 3.2. Combined treatment of fasting-mimicking and 20(S)-PPD induced more apoptosis and necrosis

Consistent with the cell death analysis results, fasting-mimicking was shown to significantly enhance 20(S)-PPD-induced apoptosis in HepG2 cells. After treated with 20(S)-PPD in the control medium, the cell apoptotic rates were  $2.66 \pm 0.62 \%$  (0  $\mu$ M),  $4.07 \pm 0.22 \%$  (5  $\mu$ M),  $4.60 \pm 0.30 \%$  (10  $\mu$ M),  $5.45 \pm 0.35 \%$  (20  $\mu$ M) for 24 h, respectively. Relatively, the cell apoptotic rates in fasting-mimicking medium with 20(S)-PPD were  $3.49 \pm 0.50 \%$  (0  $\mu$ M),  $5.94 \pm 0.31 \%$  (5  $\mu$ M),  $40.64 \pm 1.40 \%$  (10  $\mu$ M),  $68.85 \pm 6.71 \%$  (20  $\mu$ M), respectively (Fig. 2A and B). Likewise, the cell necrosis rates in control medium with 20(S)-PPD were  $0.88 \pm 0.19 \%$  (0  $\mu$ M),  $1.27 \pm 0.15 \%$  (5  $\mu$ M),  $5.16 \pm 0.08 \%$  (10  $\mu$ M),  $7.36 \pm 0.49 \%$  (20  $\mu$ M) for 24 h, respectively. While the cell necrosis rates in fasting-mimicking medium with 20(S)-PPD were  $1.31 \pm 0.21 \%$  (0  $\mu$ M),  $6.01 \pm 1.31 \%$  (5  $\mu$ M),  $9.43 \pm 0.38 \%$  (10  $\mu$ M),  $12.53 \pm 0.81 \%$  (20  $\mu$ M), respectively. Results showed that 20(S)-PPD was more effective in inducing cell apoptosis and necrosis on fasted cells as compared to controls. As expected, fasting-mimicking alone can not influence cell growth and death.

In addition, the cellular changes was first assessed by real-time holographic imaging (Fig. 2C). After 24 h exposure to 20  $\mu$ M 20(S)-PPD in fasting medium, more cells became smaller in surface area compared to that in control medium.

### 3.3. Fasting-mimicking increased the anti-metastasis effect of 20(S)-PPD *in vitro*

In order to investigate the role of fasting for regulating anti-metastasis effect of 20(S)-PPD on HepG2 cell migration and invasion, a key event in carcinogenesis, we performed the transwell assay. As depicted in Fig. 3A and B, the 20(S)-PPD and fasting-mimicking-treated groups exhibited a more potent effect on the inhibition of cell invasion. The number of invaded HepG2 cells in the control medium were  $424.00 \pm 22.70$  (0  $\mu$ M),  $338.3 \pm 24.22$  (1.25  $\mu$ M),  $224.67 \pm 8.96$  (2.5  $\mu$ M) and  $153.00 \pm 18.52$  (5  $\mu$ M), respectively. In addition, the number of invaded cells in fasting-mimicking medium were  $431.67 \pm 22.85$  (0  $\mu$ M),  $254.33 \pm 14.05$  (1.25  $\mu$ M),  $181.67 \pm 10.97$  (2.5  $\mu$ M) and  $72.00 \pm 10.44$  (5  $\mu$ M), respectively. Meanwhile, HepG2 cells exhibited significantly lower migration ability with 20(S)-PPD in fasting-mimicking medium compared to that in control medium (Fig. 3C). Moreover, the expression of matrix metalloproteinase (MMP)-2 and matrix metalloproteinase (MMP)-9 in cells treated in fasting-mimicking conditioned medium combined with 20(S)-PPD could be largely suppressed (Fig. 3D–F).

3D reconstruction imaging (Fig. 4) has an advantage for the comparison of cell volume and morphology (i.e., thickness). Acquisition of mesenchymal phenotype through EMT has been conformed to be associated with aggressive tumor subtypes and poor clinical outcome in patients. It was observed that cells in fasting-mimicking medium tended to inhibit HepG2 cell mesenchymal phenotype. Next, we tracked the movement of HepG2 cells in control medium or fasting-mimicking medium combined with 20(S)-PPD by the HoloMonitor M4 time-lapse cytometer. Time-lapse cell-tracking analysis confirmed that fasted cells showed lower random motility and speed with 20  $\mu$ M 20(S)-PPD.

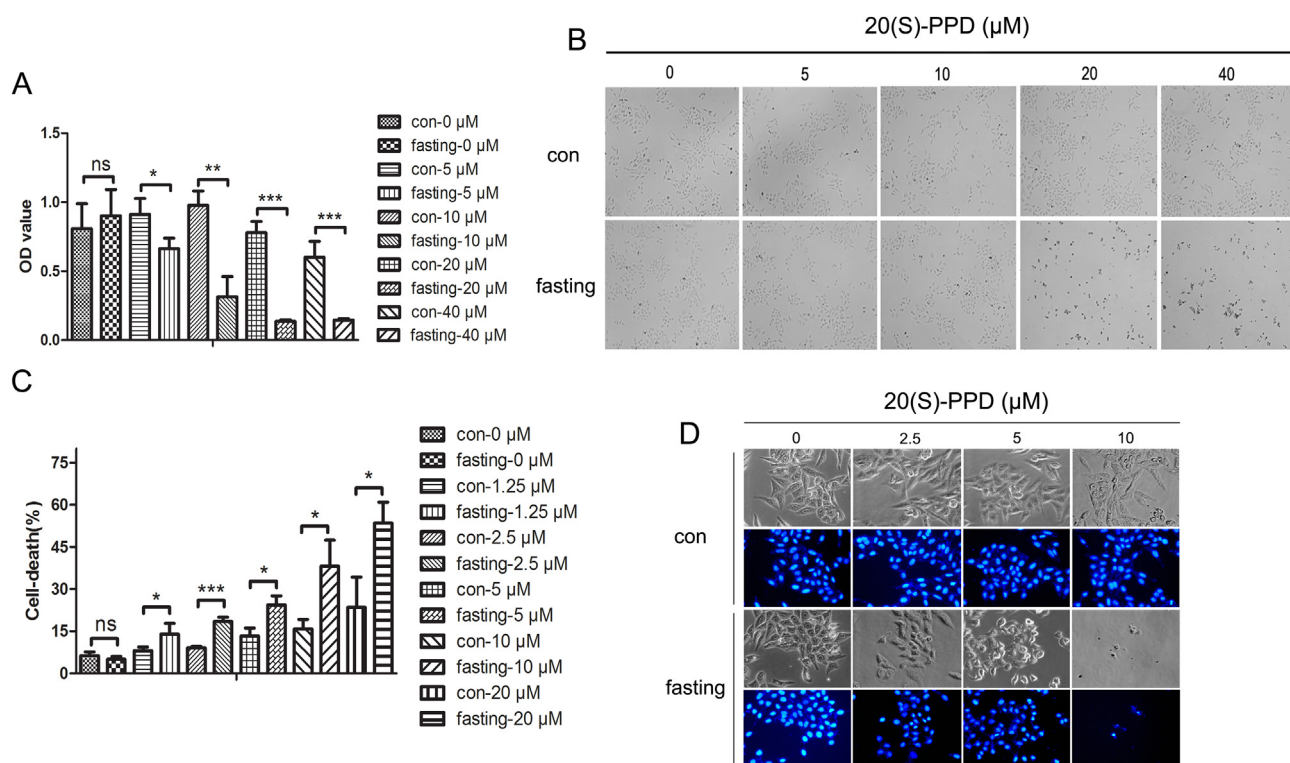


**Fig. 1.** Different concentrations of 20(S)-PPD combined with control medium and fasting-mimicking medium in HepG2 cells. (A) Anti-proliferative effect was evaluated through CCK-8 colorimetric assay. HepG2 cells cultured with 20(S)-PPD (0, 5, 10, 20 and 40 μM) were detected for 24 h. (B) Morphological changes of cells were observed and photographed under a phase contrast microscope. (C) Cell death was examined by trypan blue dye exclusion and the nucleus was stained with DAPI and observed under the fluorescence microscope (D). Differences were considered as significant when  $P < 0.05$  (\*) or  $P < 0.01$  (\*\*) or  $P < 0.001$  (\*\*\*).

### 3.4. Fasting-mimicking increased the G0-G1 phase arrest induced by 20(S)-PPD

Cell cycle derangement is one of the main tumor arrest properties of anti-tumor drugs. Exposure with 0 μM and 2.5 μM 20(S)-PPD in fasting-mimicking medium, the G0-G1 phase arrest induced by 20(S)-PPD significantly increased. In addition, S phase reduced as well. Analysis represented in Fig. 5D–E showed that HepG2 cells treated with higher concentrations of 20(S)-PPD in combined groups significantly increased the percentage of cells in G0/G1 phase, with decreased G2-M phase in cells. Cyclins are among the most important core cell cycle regulators [11]. The expressions of cyclinD1 decreased in fasted cells at the same concentrations of 20(S)-PPD (Fig. 5F and G).

### 3.5. Intermittent fasting potentiates 20(S)-PPD anti-tumor effect in the H22 tumor-bearing mice

In vivo study, 20(S)-PPD treatment alone or combined with intermittent fasting was performed. As seen from Fig. 6A, the 20(S)-PPD-alone groups had effective and dose-dependent inhibition of tumor growth. Additionally, a significant retarded progression of HCC was observed, which were perceptibly strengthened when combined with intermittent fasting. In particular, the tumor volume of mice treated by intermittent fasting condition with 60 mg/kg 20(S)-PPD was  $1.08 \pm 0.39 \text{ mm}^3$ , which was nearly decreased with that of 100 mg/kg 20(S)-PPD-alone group ( $1.58 \pm 0.15 \text{ mm}^3$ ). As seen in Fig. 6, there was no obviously side effects in intermittent fasting condition combined with 20(S)-PPD according to the weights and spleen index of mice, while the thymus index was decreased with 30 mg/kg 20(S)-PPD combined with fasting

condition. More important, intermittent fasting did not cause any abnormal in mice daily activities.

## 4. Discussion

Over the last two decades only 14.1% in 5-year survival rate have been achieved for patients with HCC, which represents one of the most aggressive tumors due to its rapid progress [12]. At present, cytotoxic chemotherapy remains the major treatment option for advanced HCC. Some patients are allowed to accept targeted therapy, such as sorafenib. However, the objective response rate (ORR) of sorafenib for advanced HCC is 5% at most [13]. Moreover, sorafenib still shows adverse effects such as poor tumor-shrinking effects and relatively high toxicity (e.g., hand-foot skin reaction) [14].

20(S)-protopanaxadiol (20(S)-PPD), a derivative of ginsenosides, is the final form of protopanaxadiol saponins metabolized by human intestinal microflora. 20(S)-PPD performs many biological functions, including differentiation regulation of neural stem cells and anti-inflammatory properties [15–17]. The major novel findings in the present study were that 20(S)-PPD performed a role in a variety of tumor inhibition. But here's the question, the effective concentration of 20(S)-PPD is relatively high. For example, It was reported that 20(S)-PPD inhibited the viability of HepG2 cell in a dose- and time-dependent manner. But the IC<sub>50</sub> values were up to 81.35, 73.5, 48.79 μM at 24, 48 and 72 h, respectively [18]. To enhance the bioavailability of 20(S)-PPD in tumors, novel, safe and effective methods are needed.

Di Tano et al proposed that fasting can improve efficacy of chemotherapy and radiotherapy for some types of tumor [7]. Moreover, emerging evidence suggests that fasting can improve

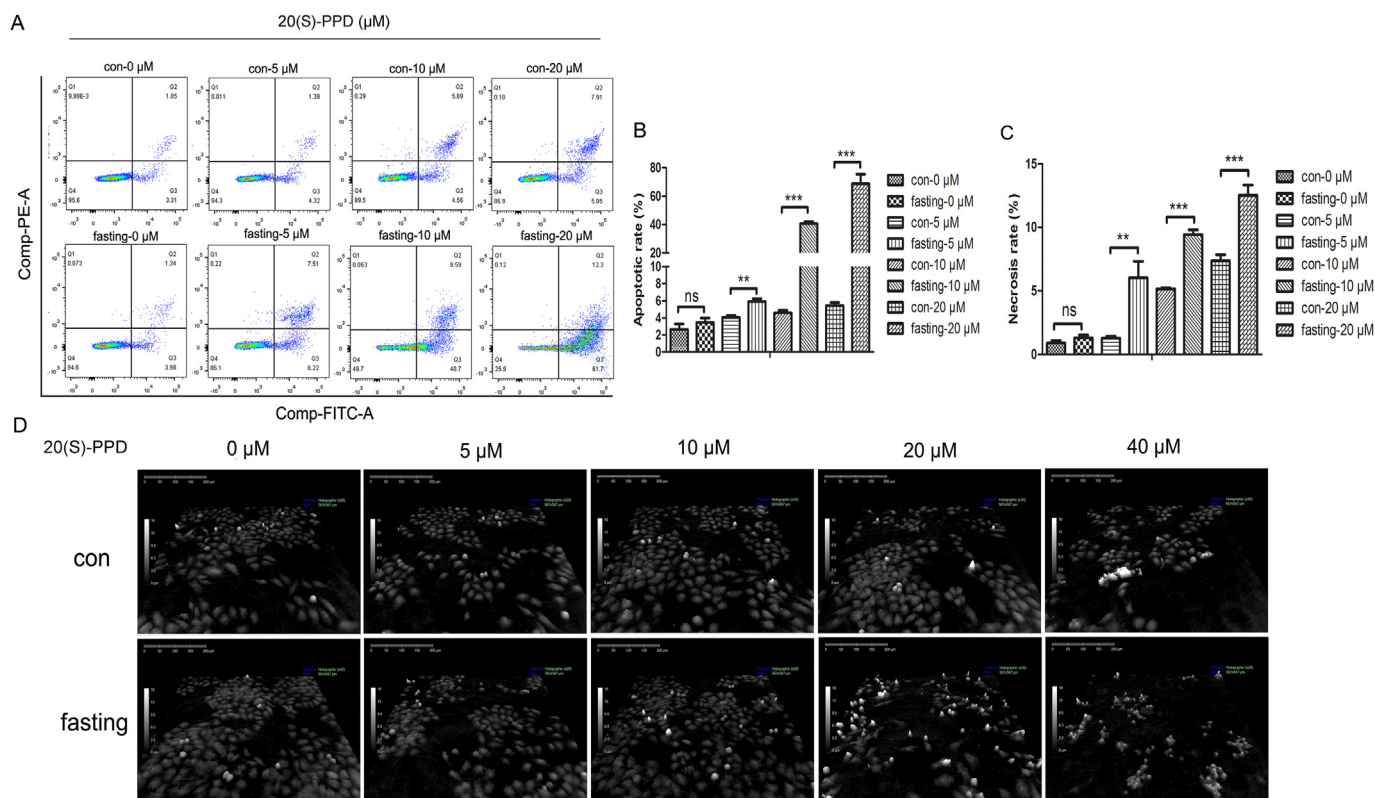


**Fig. 2.** Fasting-mimicking medium increased the apoptosis induction of 20(S)-PPD in HepG2 cells. (A) The apoptotic rates of the cells were labeled with Annexin V-FITC and PI in control medium and fasting-mimicking medium for 24 h. Apoptosis and necrosis were analyzed by a flow cytometry. Flow cytometry plots (Q4, living (AV-, PI-); Q3, apoptosis (AV+, PI-); Q2, necrotic (AV+, PI+)). (D) The cell morphology analyzed by HoloMonitorTM M4 and real-time holographic imaging were recorded at the doses indicated (24 h). Differences were considered as significant when  $P < 0.05$  (\*) or  $P < 0.01$  (\*\*) or  $P < 0.001$  (\*\*\*).

chronic inflammation by reducing the number of pro-inflammatory monocytes, reshape the immune system and improve the killing ability of T cells in tumor patients [19–21]. Therefore, we had an idea that fasting might have promising activity to enhance sensitivity to chinese medicines, such as 20(S)-PPD.

Based on this conjecture, the influences of fasting-mimicking in combination with 20(S)-PPD on human liver cancer cell line HepG2 were detected. Similar to our previous studies and other reports, 20(S)-PPD inhibited cell viability in a dose-dependent manner. The inhibition rate of 20(S)-PPD at the concentrations of 20 μM and 40 μM were  $1.61 \pm 14.13\%$  and  $21.08 \pm 33.869\%$ , respectively, while the rates of fasted cells with 20(S)-PPD were  $84.24 \pm 4.19\%$  and  $83.26 \pm 4.31\%$ . As seen from the results, the inhibition on proliferation of was 20(S)-PPD enhanced in fasting-mimicking medium.

According to the cell morphology observed under a microscope, apoptosis, one of the biological processes results in cell death, is observed by a number of typical morphological changes in the structure of the cell (Fig. 2D). Additionally, data from flow cytometry confirmed that 20(S)-PPD induced more apoptosis and necrosis in fasting-mimicking medium. Importantly, fasting-mimicking-alone treatment did not show any significant effects on proliferation and death of HepG2 cells.

In addition to the expected effect of fasting-mimicking on cell proliferation, another interesting phenotype emerged from our digital holographic analysis. Fasted cells were significantly less motile compared with control cells and showed more sensitive to the inhibition of 20(S)-PPD on cell motility. And the results of transwell assay was also as the same as imaging figures. Mechanistically, MMP-2 and MMP-9 are important regulators of invasion and the effect of fasting-mimicking on their expression levels was

also examined [22]. In fasting-mimicking medium, 20(S)-PPD inhibited invasion by decreasing more expressions of MMP-2 and MMP-9.

Then, we test the cell cycle and confirmed that fasting-mimicking increased the cell cycle arrest induced by 20(S)-PPD. Cyclin-dependent kinase 2 (CDK2) is a key cell cycle regulator, with roles in controlling both G1/S and G2/M transitions [23]. In order to promote cell cycle progression, CDK has been described to play a positive role in cell cycle arrest [24]. In fasting-mimicking medium, the expression of CDK2 diminished more with 20(S)-PPD treatment. Collectively, all these data have showed that fasting-mimicking may constituting a promising strategy for 20(S)-PPD against hepatocellular carcinoma *in vitro*.

At last, to further explore the antitumoral action of fasting-20(S)-PPD combination in an *in vivo* model, H22 cell line was injected in mice. On the 21st day after treatment, all mice were sacrificed and solid tumors were collected. The reduction of tumor growth of intermittent fasting-20(S)-PPD showed a higher efficacy than single 20(S)-PPD administration, with no toxicity concerns, what supports the potential use of the combination *in vivo*. The weight and volume of tumors were both smaller in intermittent fasting groups compared to that treated with 20(S)-PPD alone on the same concentrations. Moreover, the body weight of the intermittent fasting-20(S)-PPD-treated mice was not significantly different from its 20(S)-PPD-treated mice. No signs of acute lethal toxicity, weight loss or behavioral changes were observed in treated mice during intermittent fasting cycles. It was worthy of note that intermittent fasting combined with anti-tumor agents tended to reduce tumor mass, which might represent an alternative for patients who are unable to undergo these conventional treatments.

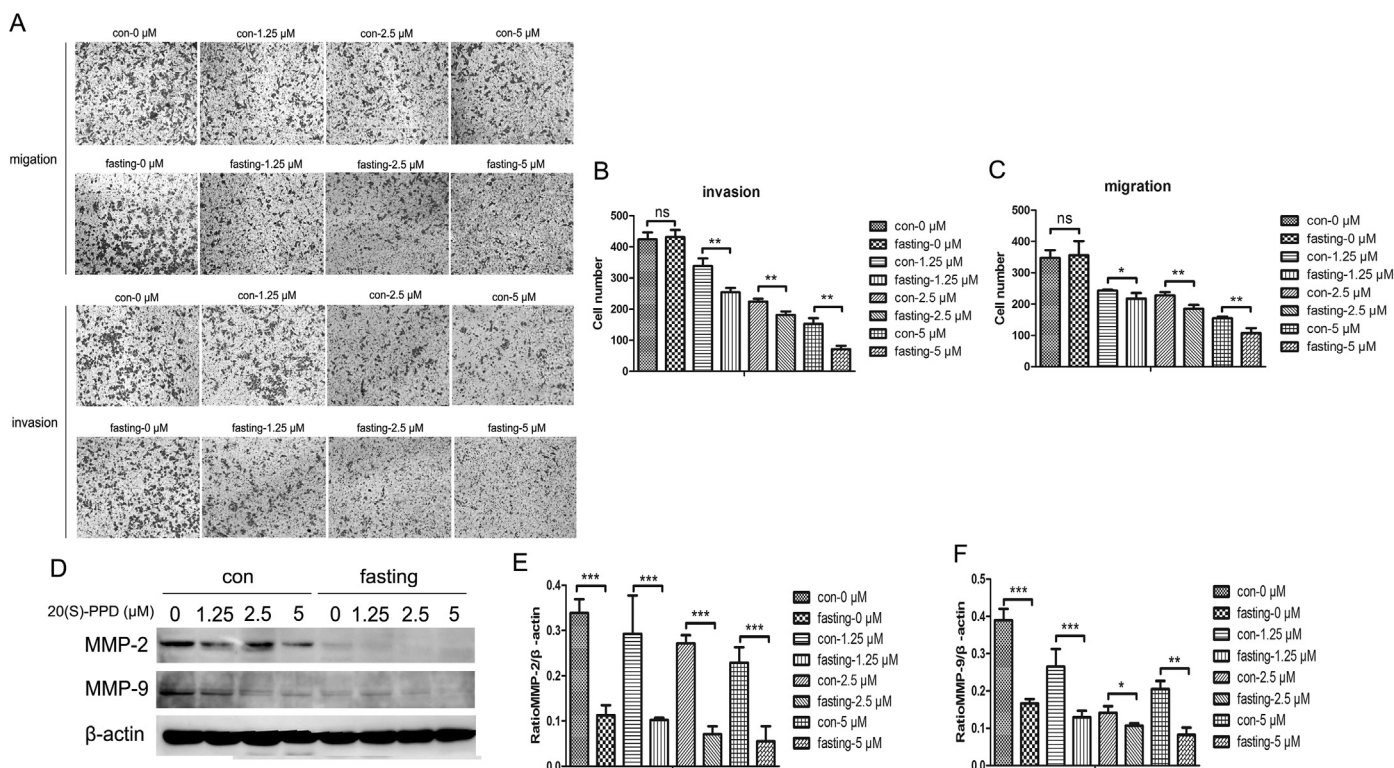


**Fig. 3.** Cell migration and invasion were detected by transwell chamber assays. (A–C) Cell number of invasive and migratory cells were calculated. The magnification is 200 × . (D–F) MMP-2 and MMP-9 protein expressions were evaluated by western blot analysis in the control medium and fasting-mimicking medium for 24 h. β-actin was used as a loading control. \**P* < 0.05, \*\**P* < 0.01, \*\*\**P* < 0.001 vs control group.

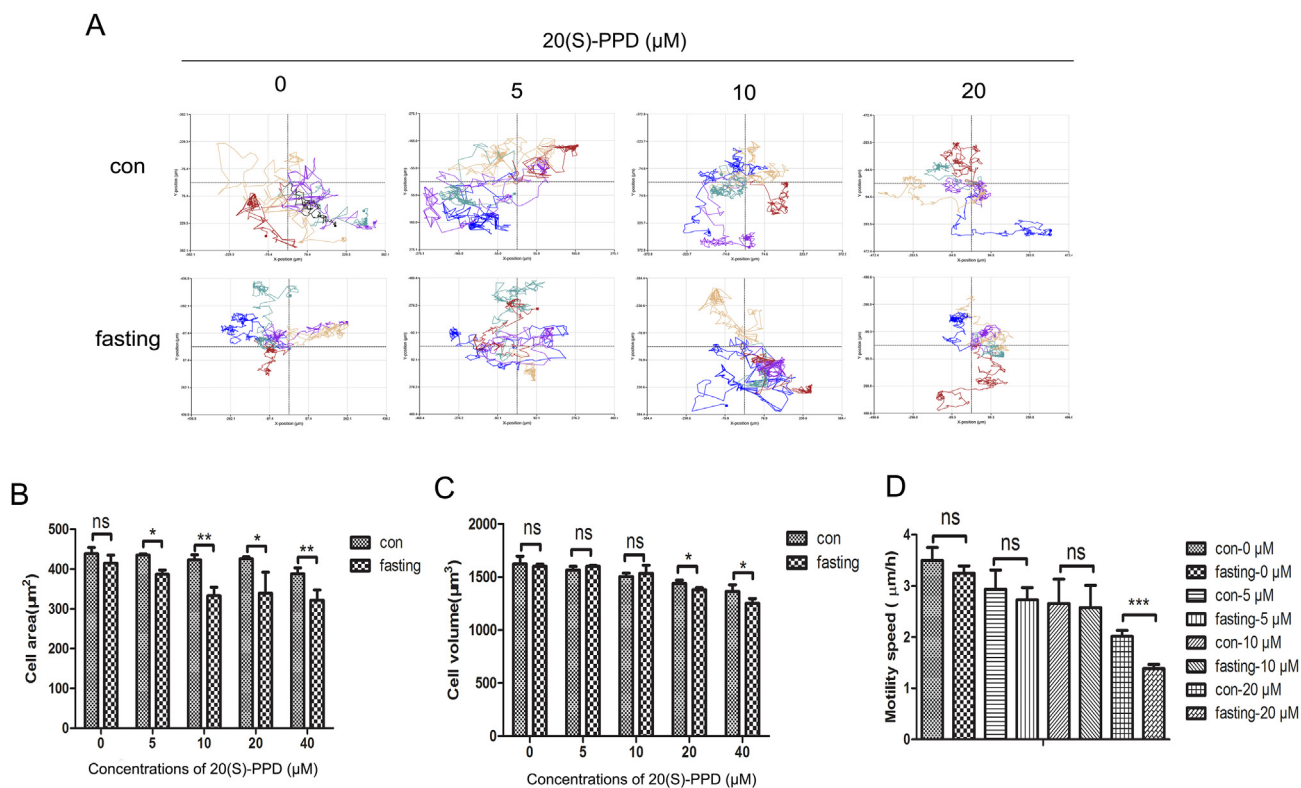


**Fig. 4.** The motility was analyzed by real-time holographic imaging.(A) The range of cell movement was analyzed. And the area and volume of cells were also analyzed by HoMonitor™ M4(B–C). (D) Motility speed of cells were analyzed. Differences were considered as significant when *P* < 0.05 (\*) or *P* < 0.01 (\*\*) or *P* < 0.001 (\*\*\*).

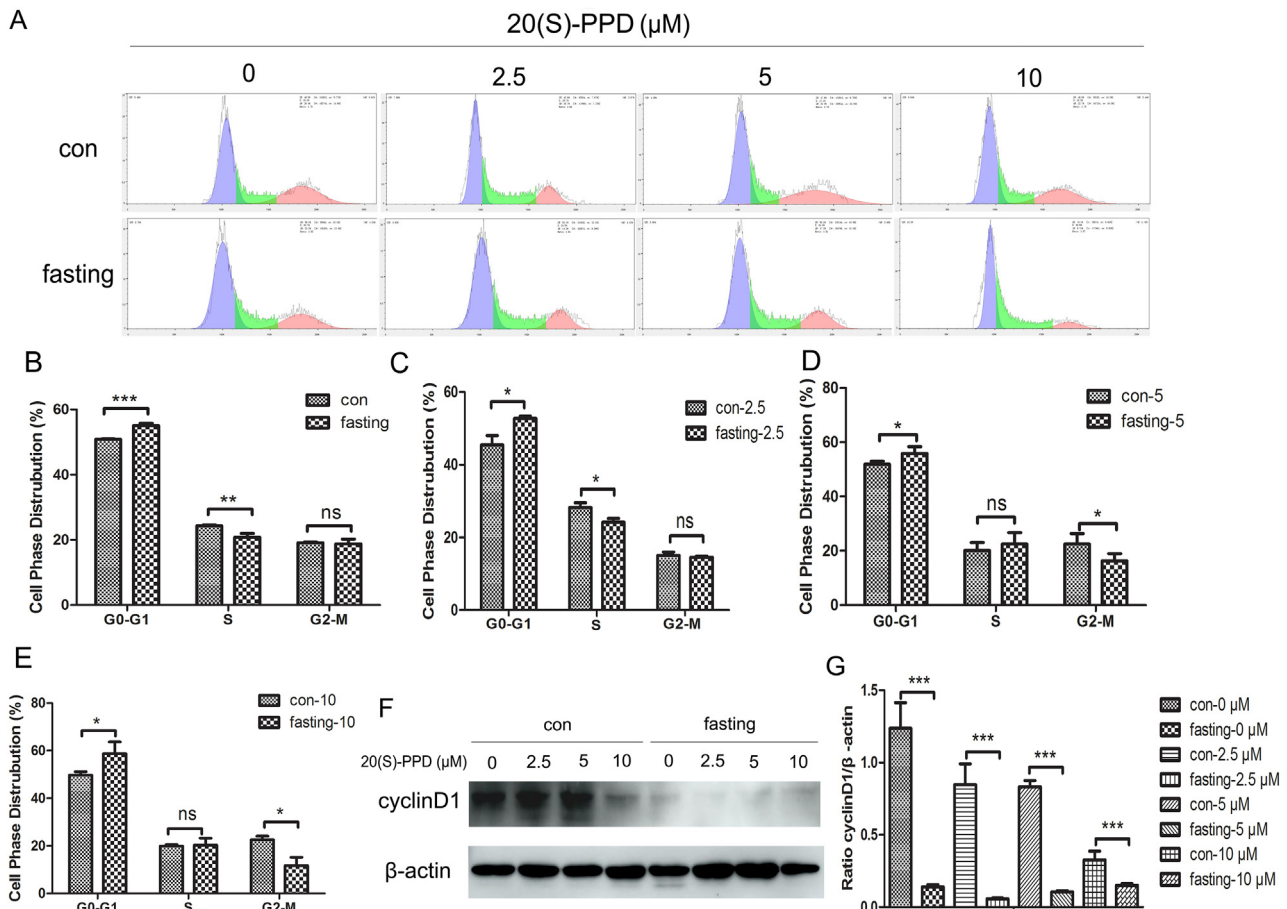


**Fig. 5.** Fasting enhanced the G0-G1 phase arrest of 20(S)-PPD in HepG2 cells compared with control exposure. (A) Cell cycle phase distribution in HepG2 cells were analyzed by a flow cytometer. (B-E) The percentage of cells at G0-G1, S and G2-M phases were presented. (F-G) Western blot assay was conducted to measure the protein levels of cyclinD1. The intensity of proteins was quantified by QuantityOne software. Data were the mean  $\pm$  SD of independent, triplicate experiments. \* represents  $P < 0.05$ , \*\* $P < 0.05$ , \*\*\* $P < 0.01$ , \*\*\* $P < 0.001$ , ns no significant differences vs control group.

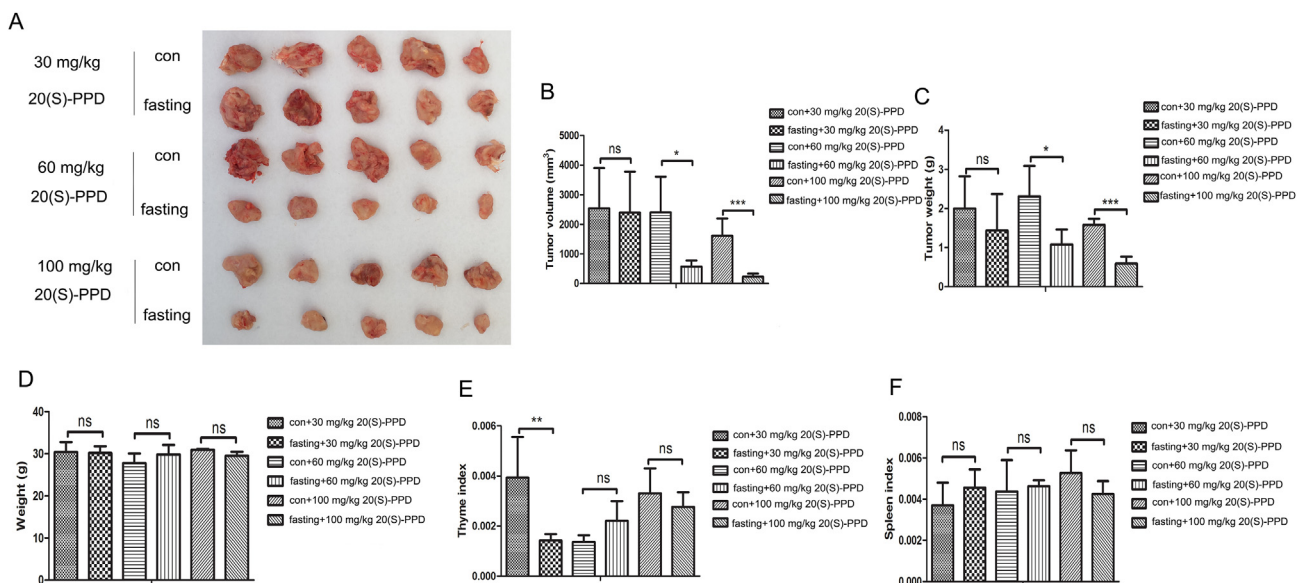


**Fig. 6.** Effects of intermittent fasting combined with 20(S)-PPD on H22 tumor-bearing mice. (A-C) The tumor mass after treatment. Tumor volume and weight expressed as the mean  $\pm$  SD in 5 mice in each group. (D) The weight of mice were examined and analyzed. (E-F) Spleen index and thymus index were examined and compared from each group. \* $P < 0.05$ , \*\* $P < 0.05$ , \*\*\* $P < 0.01$ , \*\*\* $P < 0.001$ .

Based on the results of *in vitro* and *in vivo* experiments, our results provided an experimental foundation that fasting promoted anti-tumor effects of 20(S)-PPD, suggesting that restrictive dietary interventions might be a potential strategy for treatments against hepatocellular carcinoma. These extensively findings pave the way for future fasting studies in clinical treatment of tumors.

### Declaration of competing interest

There is no conflict of interest.

### Acknowledgements

The study was supported by the grants from the Shandong Provincial Natural Science Foundation of China (ZR2018LH013), the Key Research and Development Plan of Yantai City (2019XDZH098), the National Natural Science Foundation of China (81703846).

### References

- [1] Global Burden of Disease Liver Cancer C, Akinyemiju T, Abera S, Ahmed M, Alam N, Alemayohu MA, Allen C, Al-Raddadi R, Alvis-Guzman N, Amoako Y, et al. The burden of primary liver cancer and underlying etiologies from 1990 to 2015 at the global, regional, and national level: results from the global burden of disease study 2015. *JAMA Oncol* 2017;3:1683–91.
- [2] Allemani C, Matsuda T, Di Carlo V, Harewood R, Matz M, Niksic M, Bonaventure A, Valkov M, Johnson CJ, Esteve J, et al. Global surveillance of trends in cancer survival 2000–14 (CONCORD-3): analysis of individual records for 37 513 025 patients diagnosed with one of 18 cancers from 322 population-based registries in 71 countries. *Lancet* 2018;391:1023–75.
- [3] De Mattia E, Cecchin E, Guardascione M, Foltran L, Di Raimo T, Angelini F, D'Andrea M, Toffoli G. Pharmacogenetics of the systemic treatment in advanced hepatocellular carcinoma. *World J Gastroenterol* 2019;25:3870–96.
- [4] Rimassa L, Pressiani T, Merle P. Systemic treatment options in hepatocellular carcinoma. *Liver Cancer* 2019;8:427–46.
- [5] Peng B, He R, Xu Q, Yang Y, Hu Q, Hou H, Liu X, Li J. Ginsenoside 20(S)-protopanaxadiol inhibits triple-negative breast cancer metastasis *in vivo* by targeting EGFR-mediated MAPK pathway. *Pharmacol Res* 2019;142:1–13.
- [6] Wang CZ, Zhang Z, Wan JY, Zhang CF, Anderson S, He X, Yu C, He TC, Qi LW, Yuan CS. Protopanaxadiol, an active ginseng metabolite, significantly enhances the effects of fluorouracil on colon cancer. *Nutrients* 2015;7:799–814.
- [7] Di Tano M, Raucci F, Vernieri C, Caffa I, Buono R, Fanti M, Brandhorst S, Curigliano G, Nencioni A, de Braud F, et al. Synergistic effect of fasting-mimicking diet and vitamin C against KRAS mutated cancers. *Nat Commun* 2020;11:2332.
- [8] Caffa I, Spagnolo V, Vernieri C, Valdemarin F, Becherini P, Wei M, Brandhorst S, Zucal C, Driehuis E, Ferrando L, et al. Fasting-mimicking diet and hormone therapy induce breast cancer regression. *Nature* 2020;583:620–4.
- [9] Safdie F, Brandhorst S, Wei M, Wang W, Lee C, Hwang S, Conti PS, Chen TC, Longo VD. Fasting enhances the response of glioma to chemo- and radiotherapy. *PLoS One* 2012;7:e44603.
- [10] McClure CD, Zhong W, Hunt VL, Chapman FM, Hill FV, Priest NK. Hormesis results in trade-offs with immunity. *Evolution* 2014;68:2225–33.
- [11] Liu B, Li X, Sun F, Tong X, Bai Y, Jin K, Liu L, Dai F, Li N. HP-CagA+ regulates the expression of CDK4/CyclinD1 via reg3 to change cell cycle and promote cell proliferation. *Int J Mol Sci* 2019;21.
- [12] Khemlina G, Ikeda S, Kurzrock R. The biology of Hepatocellular carcinoma: implications for genomic and immune therapies. *Mol Cancer* 2017;16:149.
- [13] Cheng AL, Kang YK, Chen Z, Tsao CJ, Qin S, Kim JS, Luo R, Feng J, Ye S, Yang TS, et al. Efficacy and safety of sorafenib in patients in the Asia-Pacific region with advanced hepatocellular carcinoma: a phase III randomised, double-blind, placebo-controlled trial. *Lancet Oncol* 2009;10:25–34.
- [14] Kudo M. Recent advances in systemic therapy for hepatocellular carcinoma in an aging society: 2020 update. *Liver Cancer* 2020;9:640–62.
- [15] Lin K, Liu B, Lim SL, Fu X, Sze SC, Yung KK, Zhang S. 20(S)-protopanaxadiol promotes the migration, proliferation, and differentiation of neural stem cells by targeting GSK-3beta in the Wnt/GSK-3beta/beta-catenin pathway. *J Ginseng Res* 2020;44:475–82.
- [16] Jiang N, Jingwei L, Wang H, Huang H, Wang Q, Zeng G, Li S, Liu X. Ginsenoside 20(S)-protopanaxadiol attenuates depressive-like behaviour and neuroinflammation in chronic unpredictable mild stress-induced depressive rats. *Behav Brain Res* 2020;393:112710.
- [17] Jo H, Jang D, Park SK, Lee MG, Cha B, Park C, Shin YS, Park H, Baek JM, Heo H, et al. Ginsenoside 20(S)-protopanaxadiol induces cell death in human endometrial cancer cells via apoptosis. *J Ginseng Res* 2021;45:126–33.
- [18] Lu Z, Xu H, Yu X, Wang Y, Huang L, Jin X, Sui D. 20(S)-Protopanaxadiol induces apoptosis in human hepatoblastoma HepG2 cells by downregulating the protein kinase B signaling pathway. *Exp Ther Med* 2018;15:1277–84.
- [19] Jordan S, Tung N, Casanova-Acebes M, Chang C, Cantoni C, Zhang D, Wirtz TH, Naik S, Rose SA, Brocker CN, et al. Dietary intake regulates the circulating inflammatory monocyte pool. *Cell* 2019;178:1102–1114 e1117.
- [20] Brandhorst S, Choi IY, Wei M, Cheng CW, Sedrakyan S, Navarrete G, Dubeau L, Yap LP, Park R, Vinciguerra M, et al. A periodic diet that mimics fasting promotes multi-system regeneration, enhanced cognitive performance, and healthspan. *Cell Metab* 2015;22:86–99.
- [21] Di Biase S, Lee C, Brandhorst S, Manes B, Buono R, Cheng CW, Cacciottolo M, Martin-Montalvo A, de Cabo R, Wei M, et al. Fasting-mimicking diet reduces HO-1 to promote T cell-mediated tumor cytotoxicity. *Cancer Cell* 2016;30:136–46.
- [22] Li Z, Takino T, Endo Y, Sato H. Activation of MMP-9 by membrane type-1 MMP/MMP-2 axis stimulates tumor metastasis. *Cancer Sci* 2017;108:347–53.
- [23] Liu Q, Liu X, Gao J, Shi X, Hu X, Wang S, Luo Y. Overexpression of DOC-1R inhibits cell cycle G1/S transition by repressing CDK2 expression and activation. *Int J Biol Sci* 2013;9:541–9.
- [24] Bacevic K, Lossaint G, Achour TN, Georget V, Fisher D, Dulic V. Cdk2 strengthens the intra-S checkpoint and counteracts cell cycle exit induced by DNA damage. *Sci Rep* 2017;7:13429.